Stanisława Jonas, Jadwiga Konefał-Góral*, Anna Małek, Stanisława Kluska and Zbigniew Grzesik

Surface Modification of the Ti6Al4V Alloy with Silicon Carbonitride Layer Deposited by PACVD Method

Abstract: Four different layers of various silicon, carbon and nitrogen contents on the Ti6Al4V alloy and (001)Si wafers have been deposited by means of Plasma Assisted Chemical Vapor Deposition (PACVD) method. The layers were obtained from reactive gas mixture containing SiH_4, CH_4, NH_3 and Ar. After deposition the structure and chemical composition of modified surfaces have been analyzed with use of SEM/EDS technique. Based on these results and thermodynamic calculations, the diffusion coefficients, D, for nitrogen and carbon in alloy were discussed. Scratch test shown that silicon carbonitride layers have good adhesion to metal surface. In order to determine atomic structure of obtained layers, FTIR spectra for layer-(001)Si and layer-Ti6Al4V were registered.

Keywords: $SiC_xN_y(H)$ layers, PACVD method, Ti6Al4V, scratch test

PACS® (2010). 81.15.Gh

***Corresponding author: Jadwiga Konefał-Góral:** Faculty of Materials Science and Ceramics, AGH University of Science and Technology, Krakow 30-059, Poland. E-mail: konefal@agh.edu.pl
Stanisława Jonas, Anna Małek, Stanisława Kluska, Zbigniew Grzesik: Faculty of Materials Science and Ceramics, AGH University of Science and Technology, Krakow 30-059, Poland

1 Introduction

One way of obtaining new materials with different properties is to modify existing ones to improve their insufficient properties. Due to the fact that many of the useful properties of the Ti6Al4V alloy, including wear and corrosion resistance, friction coefficient and biocompatibility, depend on the state of the surface, modern surface engineering methods are especially helpful. According to literature [1–3], there are many methods to improve the corrosion resistance, mechanical properties and osseointegration of titanium-based implants. Mechanical methods such as machining, grinding, polishing, consist of the physical treatment and thereby forming a suitable surface topography and its roughness, the removal of surface contamination and/or improving the adhesion of the subsequent stages of physical or chemical modification. The specificity of physical methods, such as thermal spray, PVD method or ion implantation, is the absence of chemical reactions. In this case, the layers on substrate surface are created mainly using the thermal or kinetic energy. Next group of methods, used to improve insufficient properties of titanium, contains chemical methods. The most important methods are: treatment with an appropriate chemical environment, anodic oxidation, sol-gel methods and diverse group of chemical vapor deposition (CVD), and biochemical modification. During chemical or electrochemical treatments and biochemical modifications, chemical, electrochemical or biochemical reactions occur, respectively, at the interface between titanium and a solution [2]. All these methods have advantages and limitations, but in the case of titanium based materials, PACVD method is one of the most effective methods. This technique allows on obtaining layers with good adhesion to the substrates at relatively low temperatures [4, 5].

This paper presents the results of surface modification of the Ti6Al4V alloy by silicon nitride $Si_xN_y(H)$, silicon carbonitride $SiC_xN_y(H)$, silicon carbide $SiC_x(H)$ layers in respect to their chemical composition and structure.

2 Experimental procedure

The series of different layers were obtained by Chemical Vapor Deposition using microwave plasma (MWCVD 2.45 GHz, 2 kW) on (001)Si and Ti6Al4V ELI alloy. Before deposition process, the substrates were pre-cleaned with acetone. The formation of the layers was preceded by ion etching in argon plasma. The layers were deposited using the reactive gas mixture containing silane SiH_4, ammonia NH_3 and methane CH_4 at various ratios. Argon was used as inert gas. Silane and argon flows were kept at constant level. The $[NH_3]/[CH_4]$ ratio was changed in the respective experiments, while the sum of the flows of these gases was constant. In this way, four series of the samples were

Table 1: The parameters of the deposition process applied in MWCVD system during deposition of layers.

Process	Series	Layer	Gas flow (cm^3/min)				Pressure (Pa)	Power (W)	Temperature deposition (K)	Time deposition (s)
			Ar	NH_3	CH_4	SiH_4				
Ion-etching	1–4	–	225	–	–	3	40	400	293	600
Deposition	1	$Si_xN_y(H)$	225	150	–	–	40	400	873	1800
	2	$SiC_xN_y(H)$	225	140	10	3	40	400	873	1800
	3	$SiC_xN_y(H)$	225	130	20	3	40	400	873	1800
	4	$SiC_x(H)$	225	–	25	3	40	400	873	1800

obtained – each one of various silicon, carbon, nitrogen and hydrogen contents. The parameters of the deposition process applied in each series, during ion-etching and layer deposition is given in Table 1.

The chemical composition of deposited layers was determined using SEM/EDS technique (FEI Nova Nano SEM 200 with Genesis energy dispersive X-ray microprobe). Based on this method, surface distribution of the elements on deposited layers as well as their thickness were also determined. SEM studies supplemented by images made by scanning laser microscope (Keyence VK 9000). Scratch tests for $SiC_xN_y(H)$ layer and the unmodified alloy using Micro-Combi-Tester (MCT) were also done. Test parameters were chosen as follows: the load range 0–30 N, scratch test length 3 mm. The layers structure were determined based on FTIR spectroscopy. Measurements were made for the layers obtained on a (001)Si substrate and on metal. In the first case, the reference spectrum was obtained using transmission technique and in the case of metal, the reflective techniques were used (Bruker Vertex 70V spectrometer).

3 Results and discussion

The SEM studies of obtained systems included analysis of images taken for alloy samples before and after deposition process. All the samples do not differ significantly. In all images of Ti6Al4V surface only characteristic lines occur, being the result of mechanical polishing of raw metals. Such images are typical for the amorphous layers or poorly crystalline ones. Image for $SiC_xN_y(H)$/alloy system, presented in Fig. 1, obtained using scanning laser microscopy technique, shows clear evidence of the change of morphology between alloy before and after modification.

Fig. 2 shows the distribution of several elements on the modified surfaces obtained in series 1–4 (see Table 1). The images show strong effects associated with Ti6Al4V in the form of signals from Ti, Al and V, which indirectly shows that the thickness of the layers does not exceed the thickness of penetration of the electron (1 μm).

The relationships characterizing chemical composition of the deposited layers were estimated from EDS spectra. This measurements shown that when the content

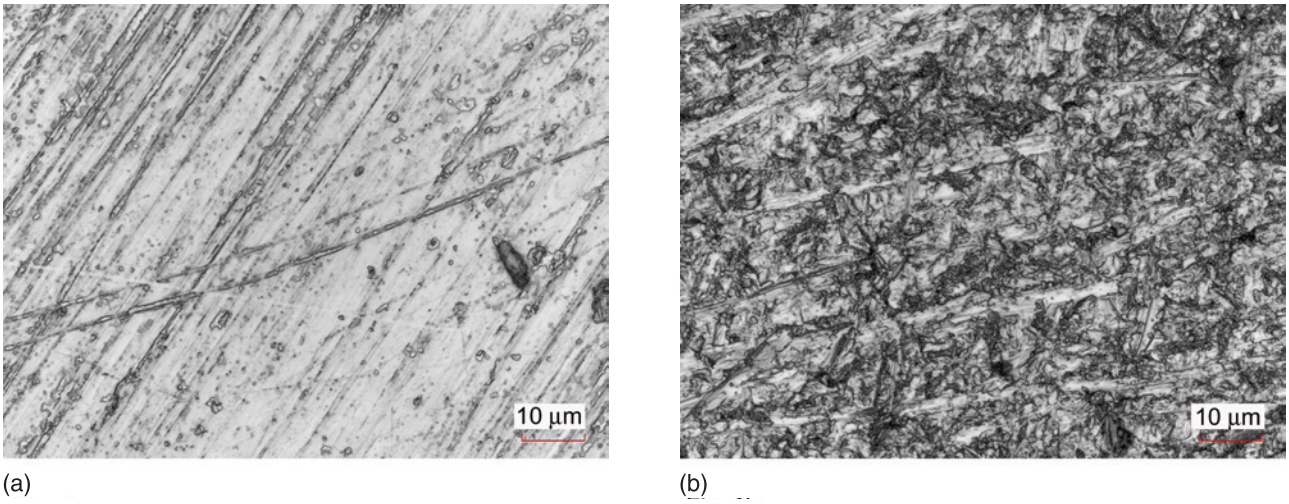

(a) (b)

Fig. 1: Scanning laser microscopy images for alloy: a) before modification, b) modified with $SiC_xN_y(H)$ layer (series 3).

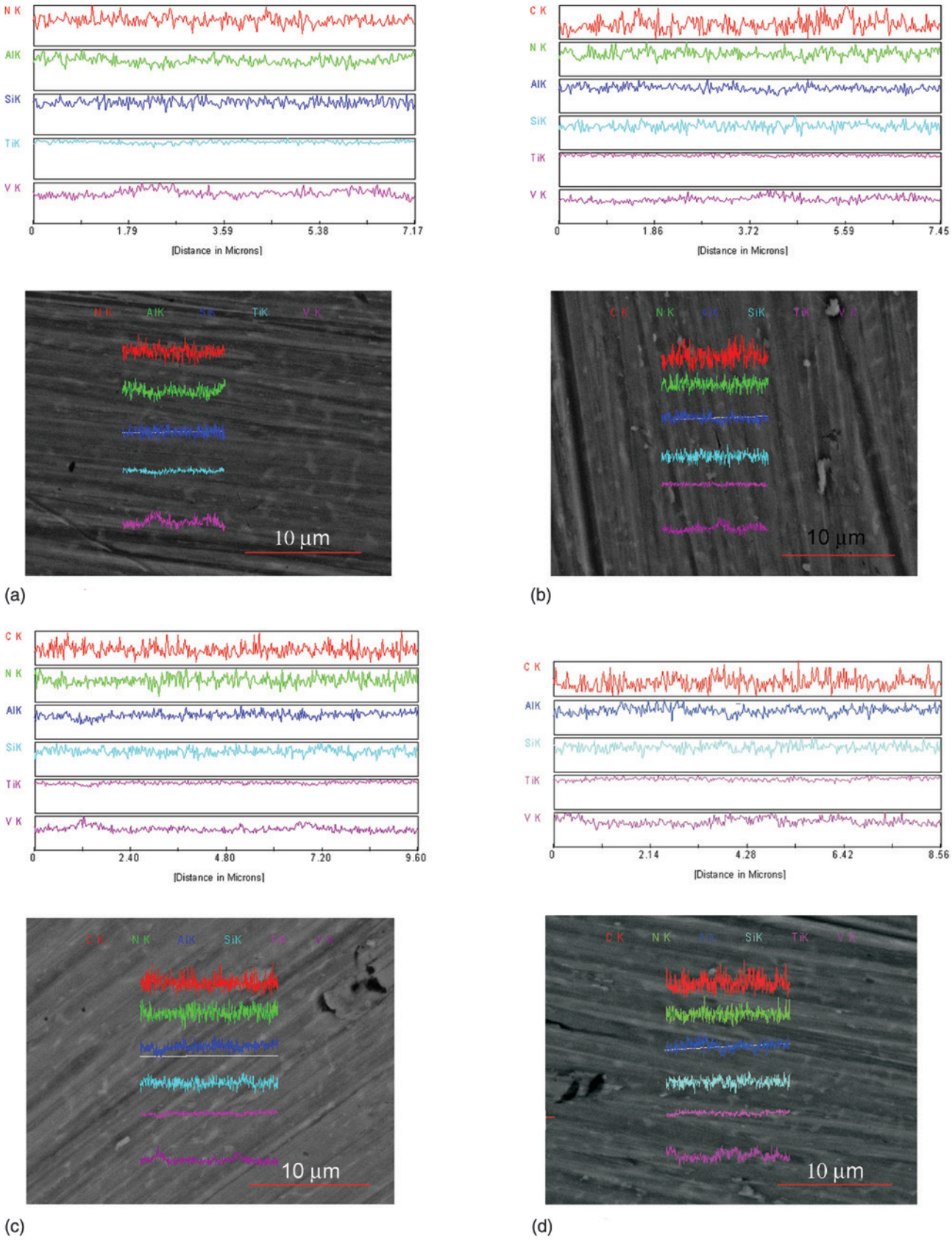

Fig. 2: The linear distribution of elements in the layers: a) Si_xN_y(H)-series 1, b) SiC_xN_y(H)-series 2, c) SiC_xN_y(H)-series 3, d) SiC_x(H)-series 4.

Table 2: Average thickness of deposited layers.

Series	Layer	Thickness (nm)
1	$Si_xN_y(H)$	120±12.62
2	$SiC_xN_y(H)$	132±18.00
3	$SiC_xN_y(H)$	122±16.35
4	$SiC_x(H)$	219±36.55

of methane in the gaseous mixture increases the contents of carbon in the coating also increases.

As already mentioned, analysis of the obtained results strongly suggests that the thickness of the deposited layers does not exceed 1 μm. This conclusion was verified by measurements of deposited layer thickness on cross-sections (Table 2). These measurements which proved unequivocally that the thickness of the layers is much less than 1 μm and it is in the range between 120 nm and 219 nm. According to author's experience, layers with thickness greater than 0.5 μm have bad adhesion to the substrate. This is understandable due to the difference in thermal expansion coefficients (α) of the deposited layer and substrate (i.e. titanium alloy). This coefficient for the titanium alloy is equal $2.4 \cdot 10^{-6}$ 1/°C [2]. In the case of the silicon carbonitride layers, the thermal expansion coefficient has been estimated taking the average value of amorphous Si_3N_4 ($4.5 \cdot 10^{-6}$ 1/°C) and SiC ($0.76 \cdot 10^{-7}$ 1/°C) [6]. Calculations show that the α value for the layers is about nine times higher than that for the Ti6Al4V substrate. Therefore the occurrence of tensile stresses in the layer is inevitable and their value may exceed the tensile strength leading to transverse cracks.

Fig. 3 shows the results of EDS analysis of elements along the line for the several layer-alloy systems. Analyzed sections pass through three phases – the resin, the layer and the substrate. In the case of small layer thickness applied in this work, compared to the diameter of the electron beam, in this analysis the signals from all of the phases are visible. The results show that on the border zone interlayer is formed which thickness is widely greater than the thickness of silicon carbonitride layer. The interlayer contains carbon for $SiC_x(H)$, nitrogen for $Si_xN_y(H)$ and for $SiC_xN_y(H)$ layer, in comparable amount, carbon and nitrogen (Fig. 3a–c). The formatting of interlayer guarantees good adhesion of layer to metallic substrate.

The obtained results require more detailed discussion of the diffusion coefficients of carbon and nitrogen in the titanium alloy and their chemical affinity for the substrates. Bregolin et al. determined the diffusion coefficient of nitrogen in titanium at temperatures ranging from 400

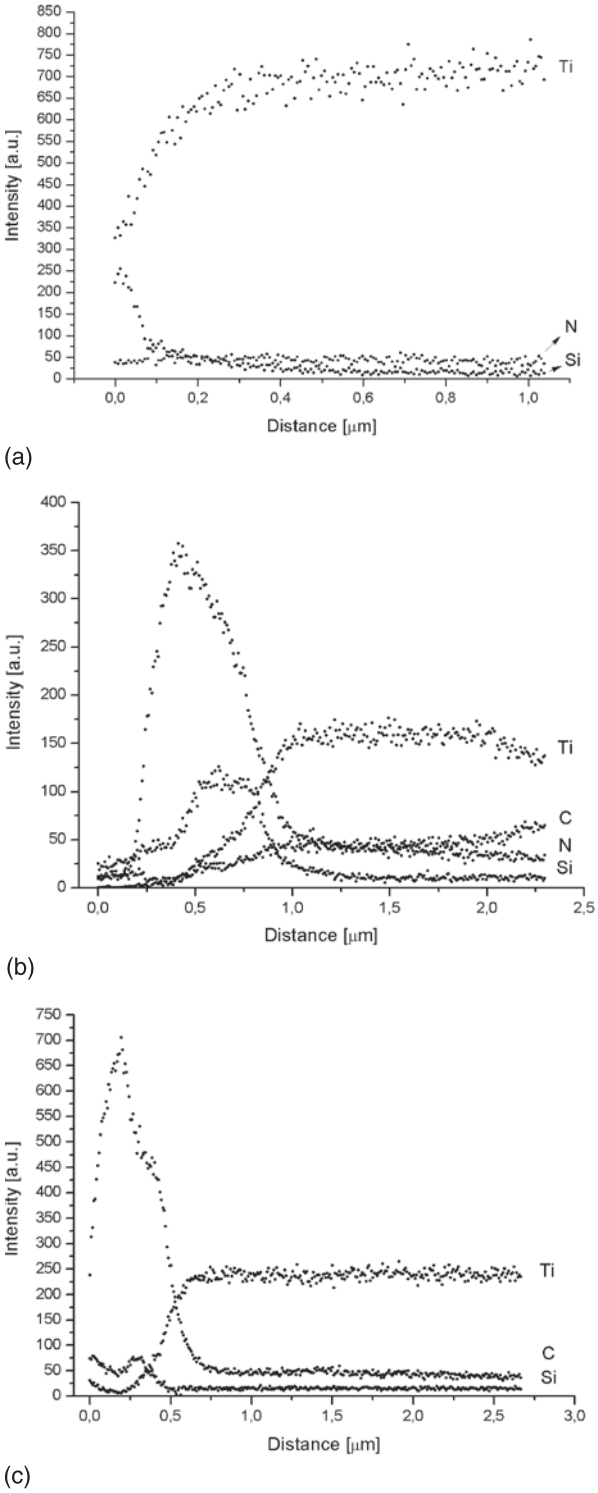

Fig. 3: SEM analysis of elements along the line determined for systems: a) $Si_xN_y(H)$/alloy, b) $SiC_xN_y(H)$/alloy, c) $SiC_x(H)$/alloy.

to 950 °C. At a temperature of 600 °C, being the deposition temperature for presented layers, diffusion coefficient of nitrogen in titanium equals $1.5 \cdot 10^{-18}$ m^2/s [7]. This result is consistent with data published by V. Fouguet et al.

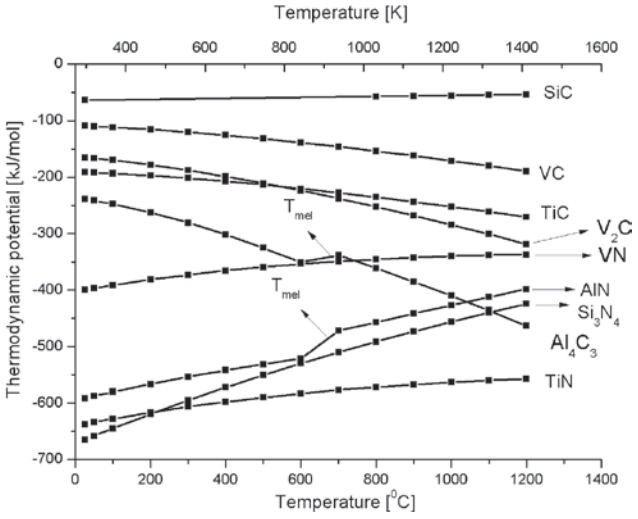

Fig. 4: Temperature dependence of thermodynamic potential for compounds forming in the C-N-Si-Ti-Al-V system (calculated on the basis of thermodynamic data [10]).

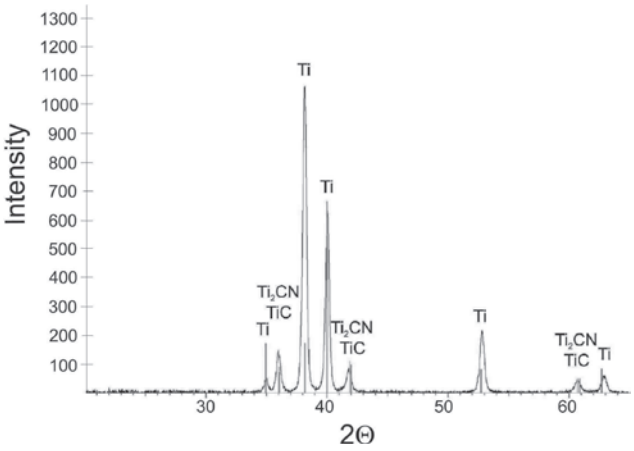

Fig. 5: XRD analysis of alloy sample with $SiC_xN_y(H)$ layer.

which contains the value of D, in the same temperature range for nitrogen in titanium and in Ti_2N, being equal to 10^{-18} m^2/s [8]. Fouguet et al. emphasize that it increases rapidly at temperatures above 500 °C. According to the data presented by other authors [9], the diffusion coefficient of carbon in titanium is higher than the diffusion coefficient of nitrogen in titanium, and equals 10^{-13} m^2/s in Ti (D of carbon in TiC equals 10^{-17} m^2/s [9]). These values are comparable for the Ti6Al4V alloy at 600 °C. Taking into account this fact lower intensity of signals from carbon than that from the nitrogen should be expected. However in the analysis shown in Fig. 3 it has not been found. Probably in such difficult a gas-solid system, where the chemical reagents (the carriers of carbon, nitrogen and silicon) are in the gas phase, on the diffusion coefficient affects the affinity of titanium relative to these elements. It should be added that in the process of layer formation the chemical reactions occur in the gas phase and on the surface of the samples. Fig. 4 shows dependence between thermodynamic potential and temperature for all possible compounds formed in discussed system. As it is shown in entire temperature range, the chemical affinity for nitrogen to all possible elements contained in the system is higher than the affinity for carbon (except Al_4C_3, which above about 1000 K has a lower affinity than TiN and AlN).

Based on the analysis of X-ray diffraction patterns obtained for alloy samples coated with $SiC_xN_y(H)$ layer, it is difficult to determine what compound of carbon and titanium dominate in the structure because these compounds are isostructural and mutually soluble, so that lines derived from them are overlapped (Fig. 5). In the XRD analysis presented at Fig. 5 there is no signals from silicon carbonitride so this layer is amorphous.

Scratch tests of selected samples (alloy before modification and $SiC_xN_y(H)$-alloy system) was carried out using Micro-Combi-Tester (MCT). Test parameters were chosen as follows: the load range 0–30 N, scratch test length 3 mm. Scratch resistance tests were carried out on sample with $SiC_xN_y(H)$ layer.

For the sample with $SiC_xN_y(H)$ removal of layer from the substrate across the width of the track at a load scratches 2 N was observed (Fig. 6a). But this layer showed very diverse adhesion to the substrate. Measurement in another area on the sample showed that the scratch resistance of silicon carbonitride layer is higher. The first small fragments are removed at a load of 5 N (Fig. 6b), and only load of 13 N lead to removal of coating from the substrate (Fig. 6d).

More information about atomic structure of layers provide FTIR spectra taken with reflective and transmission techniques for layers deposited on Ti6Al4V alloy and (001)Si surfaces, respectively. Spectrum recorded on Ti6Al4V substrate is much less intense due to the nature of the reflective technique (Figs. 7–10). The most characteristic bands are presented in Table 3. Some bands can be seen in both (001)Si and Ti6Al4V spectra. Fig. 7 ilustrates spectrum recorded for $(001)Si/Si_xN_y(H)$ system. As it is shown, the most intensive bands occur at about 835 cm^{-1} which is characteristic for Si_3N_4 and Si-N-Si [11, 12]. In the case of $Ti6Al4V/Si_xN_y(H)$ system it reveals a significant effect of the metallic substrate on the layer structure. At about 780 cm^{-1} and 990 cm^{-1} vibrations occur in the Ti-O, Ti-N and Si-N groups [13, 14]. At both spectrum vibrations in the range of 2105–2150 cm^{-1}, 2920–2970 cm^{-1} and 3230–3350 cm^{-1} are shown. They are characteristic for Si-H, CH_n (probably coming from contaminations) and NH, NH_2, N-H···N, O-H vibrations, respectively [15–19].

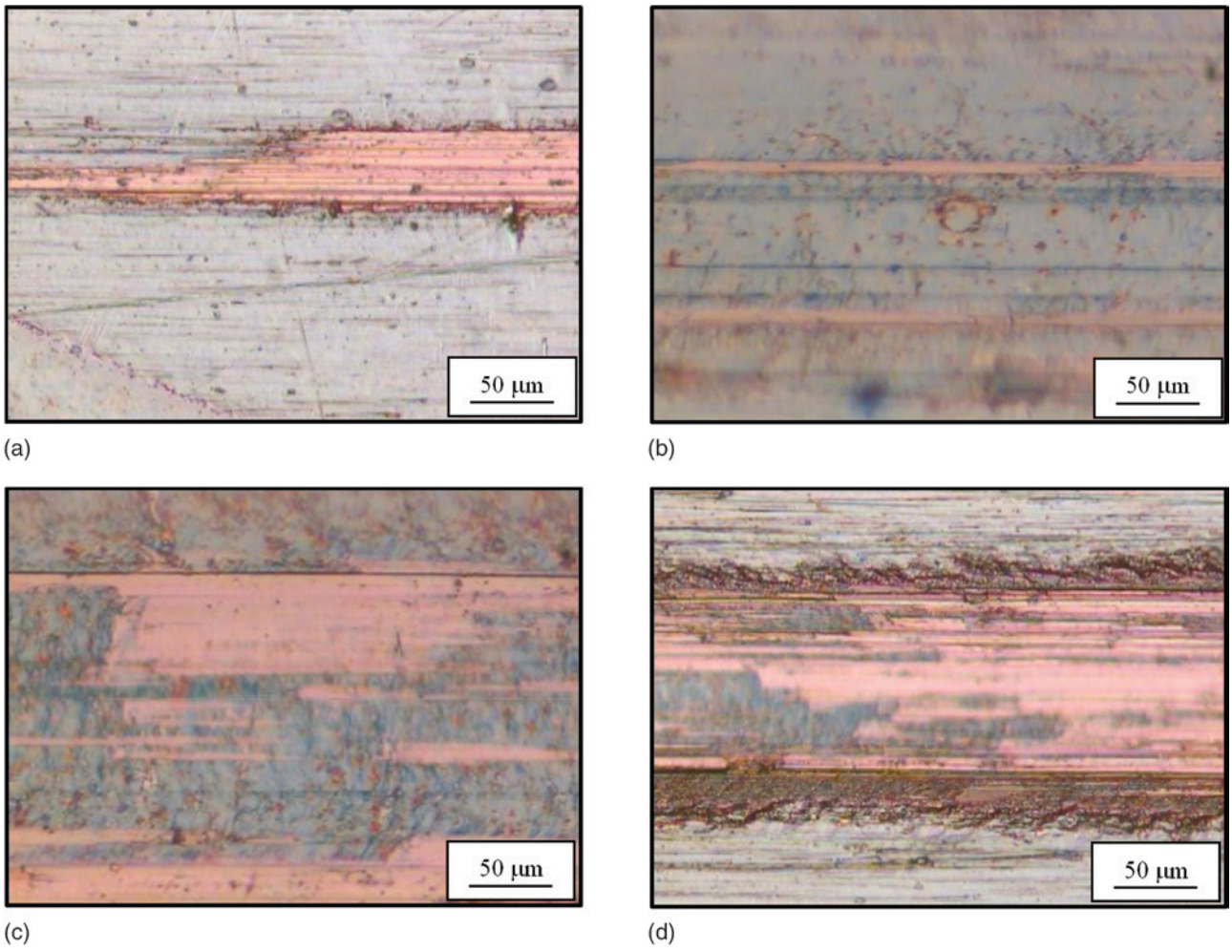

Fig. 6: Scratch track images for $SiC_xN_y(H)$/alloy system under load: a) 2 N, b) 5 N, c) 10 N, d) 13 N.

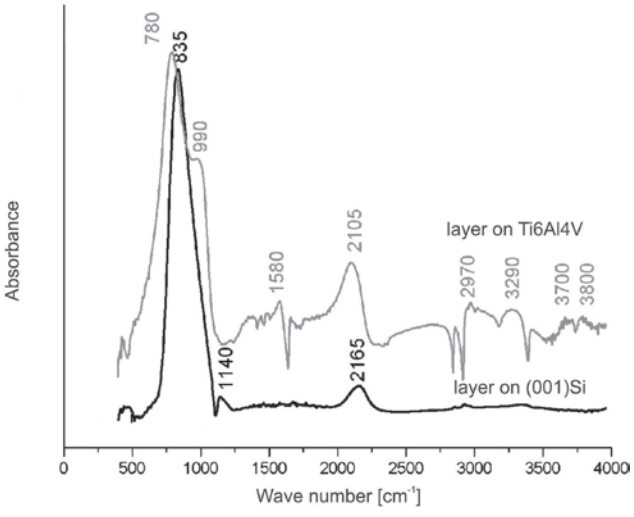

Fig. 7: FTIR spectra for $Si_xN_y(H)$/(001)Si and $Si_xN_y(H)$/alloy synthesis in series 1.

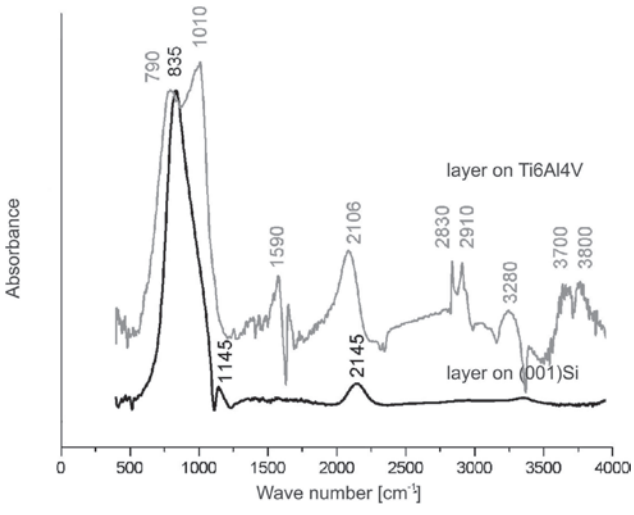

Fig. 8: FTIR spectra for $SiC_xN_y(H)$/(001)Si and $SiC_xN_y(H)$/alloy synthesis in series 2.

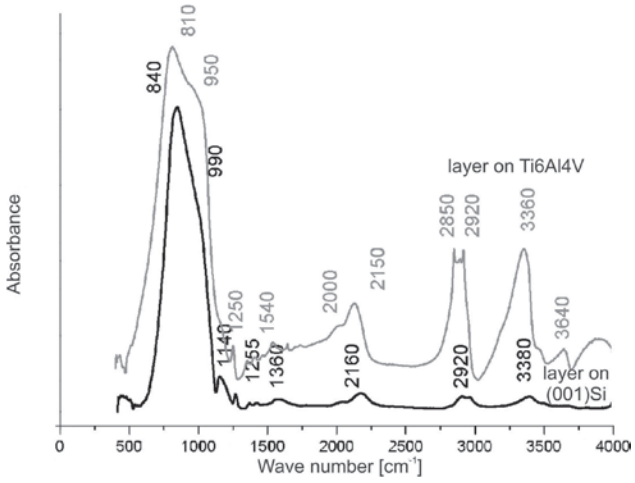

Fig. 9: FTIR spectra for $SiC_xN_y(H)$/(001)Si and $SiC_xN_y(H)$/alloy synthesis in series 3.

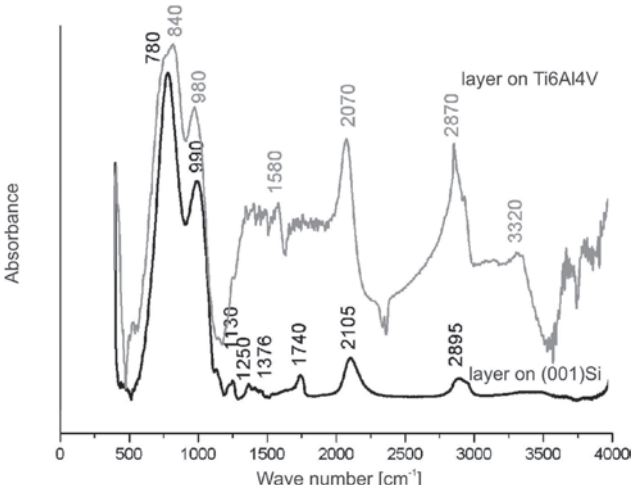

Fig. 10: FTIR spectra for $SiC_x(H)$/(001)Si and $SiC_x(H)$/alloy synthesis in series 4.

Spectra for $SiC_xN_y(H)$ layers are presented in Fig. 8. The most intensive band, for (001)Si/$SiC_xN_y(H)$ system, occurs in the range of 830–840 cm^{-1} resulting from the vibrations in the groups in which the silicon is surrounded by carbon and nitrogen (Si-C_x-N_y). In addition, vibrations around 950–990 cm^{-1}, 1250 cm^{-1}, 1540–1560 cm^{-1}, 2000–2020 cm^{-1}, 2150–2160 cm^{-1}, 2850–2950 cm^{-1} and 3340–3640 cm^{-1} come from the vibration of Si-CH_3, C-NO_2 and -OH, =C=C=N-, Si-H, CH_n, NH, NH_2, N-H, N-H···N, O-H, respectively [15–19]. Lack of vibrations characteristic for SiC in about 800 cm^{-1} and Si_3N_4 990 cm^{-1} compound proved that in the sample these phases are not present [11, 12, 15]. In the case of Ti6Al4V/$SiC_xN_y(H)$ system (Figs. 8 and 9), next to the vibrations previously interpreted, bands from Ti-O (at about 790–1010 cm^{-1}) and Ti-N (at about 1010 cm^{-1}) are visible [13, 14].

Spectra shown at Fig. 10 are characteristic for $SiC_x(H)$ layers deposited on (001)Si and alloy surfaces. Both of them are dominated by the band at about 780–980 cm^{-1} corresponding to the Si-$(CH_3)_x$ and Ti-O groups [11, 13–15]. Rest of less intensive vibration are interpreted in Table 3. Oscillation at approximately 1130–1155 cm^{-1} occurring at all spectra is an 'artificial' band resulting from the subtraction.

Table 3: Interpretation of FTIR spectra for synthesis systems [11–19].

(001)Si surface band (cm^{-1})	Assignment	Ti6Al4V surface band (cm^{-1})
–	Ti-O, Ti-N, Si-N	780, 990
840	C-Si_x-N_y	810
835	Si_3N_4, Si-N-Si	–
982–990	Si-CH_3	950–990
1246–1250	Si-$(CH_3)_x$	1250
1370	C-NO_2, O-H	–
1560	C-NO_2, C=C	1540–1590
2020	=C=C=N-	2000–2073
2096–2160	Si-H	2105–2150
2890–2950	CH_n (n = 1, 2, 3)	2830–2970
3340–3380	NH, NH_2, N-H···N, O-H	3280–3640

4 Conclusions

In the MWCVD process amorphous $Si_xN_y(H)$, $SiC_xN_y(H)$, $SiC_x(H)$ layers with chemical composition depending on the relative properties of gaseous reactants introduced into the reactor are formed. The layers thickness on alloy surface is in the range 120–219 nm. Between alloy and silicon carbonitride layer the interlayer, containing compounds of titanium with nitrogen and optionally with carbon, is formed. The $SiC_xN_y(H)$ layers have good adhesion to the substrate. The FTIR spectra showed that all deposited layers have a complex structure and the consistent elements are in bounded form. Spectra for $SiC_xN_y(H)$ layers show that the most intensive band, for (001)Si/$SiC_xN_y(H)$ system, occurs in the range of 830–840 cm^{-1} resulting from the vibrations in the groups in which the silicon is surrounded by carbon and nitrogen (Si-C_x-N_y). Next, vibrations around 950–990 cm^{-1}, 1250 cm^{-1}, 1540–1560 cm^{-1}, 2000–2020 cm^{-1}, 2150–2160 cm^{-1}, 2850–2950 cm^{-1} and 3340–3640 cm^{-1} come from the vibration of Si-CH_3, C-NO_2 and -OH, =C=C=N-, Si-H, CH_n, NH, NH_2, N-H, N-H···N, O-H, respectively. In the case of layer deposited on metallic surface in addition to the vibrations previously interpreted, bands from Ti-O (at about 790–1010 cm^{-1}) and Ti-N (at about 1010 cm^{-1}) are visible.

Received: July 2, 2013. Accepted: October 31, 2013.

References

[1] E. Krasicka-Cydzik, Formation of thin anodic layers on titanium and its implant alloys in phosphoric acid solutions, Zielona Góra University Press, 2003.

[2] X. Liu, P.K. Chu, Ch. Ding, *Mat. Sci. Eng.*, R 47 (2004) 49–121.

[3] M. Geetha, A.K. Singh, R. Asokamani, A.K. Gogia, *Prog. Mater Sci.*, 54 (2009) 397–425.

[4] K.L. Choy, *Prog. Mater Sci.*, 48 (2003) 57–170.

[5] H.O. Pierson, Handbook of chemical vapor deposition (CVD): Principles, technology, and applications, Park Ridge: Noyes Publications, 1992.

[6] G.A. Slack, S.F. Bartram, *J. Appl. Phys.*, 46 (1975) 89–98.

[7] F.L. Bregolin, M. Behar, F. Dyment, *J. Appl. Phys.* A, 90 (2009) 347–349.

[8] V. Fouguet, L. Pichon, A. Staboni, M. Drouet, *Surf. Coat. Technol.*, 186 (2004) 34–39.

[9] M.I. De Barros, D. Rats, L. Vandenbulcke, G. Farges, *Diamond Relat. Mater.*, 8 (1999) 1022–1032.

[10] I. Barin, O. Knacke, O. Kubaschewski, Thermochemical properties of inorganic substances, Berlin: Springer, 1977.

[11] M.T. Kim, J. Lee, *Thin Solid Films*, 303 (1997) 173–179.

[12] R. Gonzalez-Luna, M.T. Rodrigo, C. Jimenez, J.M. Martinez-Duart, *Thin Solid Films*, 317 (1998) 347–350.

[13] O.B. Zgalat-Lozinskii, A.V. Ragulya, V.V. Skorokhod, T.V. Tomila, I.I. Timofeeva, L.I. Klochkov, V.V. Garbuz, *Powder Metall. Met. Ceram.*, 40 (2001) 9–10.

[14] D.V. Shatansky, N.A. Gloushankova, A.N. Sheveiko, Ph.V. Kiryukhantsev-Korneev, I.A. Bashova, B.N. Mavrin, S.G. Ignatov, S.Yu. Filippovich, C. Rojas, *Surf. Coat. Technol.*, 205 (2010) 728–739.

[15] E. Vassallo, A. Cremona, F. Ghezzi, F. Dellera, L. Laguardia, G. Ambrosone, U. Coscia, *Appl. Surf. Sci.*, 252 (2006) 7993–8000.

[16] W. Kafrouni, V. Rouessac, A. Julbe, J. Durand, *J. Membr. Sci.*, 329 (2009) 130–137.

[17] S. Jonas, I. Łagosz, C. Paluszkiewicz, W.S. Ptak, *J. Mol. Struct.*, 596 (2001) 101–108.

[18] K. Kyzioł, S. Jonas, K. Tkacz-Śmiech, K. Marszałek, *Vacuum*, 82 (2008) 998–1002.

[19] B. Dischler, A. Bubenzer, P. Koidl, *Appl. Phys. Lett.*, 42 (1983) 636.